Pergamon

Geochimica et Cosmochimica Acta, Vol. 68, No. 4, pp. 917–926, 2004

0016-7037/04 $30.00 + .00

doi:10.1016/S0016-7037(03)00494-0

Chondrule textures and precursor grain size: an experimental study

R. H. HEWINS* and G. E. FOX

Dept. of Geological Sciences, Rutgers University, 610 Taylor Road, Piscataway NJ 08854, USA.

(*Received May* 8, 2003; *accepted in revised form July* 17, 2003)

Abstract—Chondrule formation appears to have been a major event in the early solar system, but chondrule properties do not allow us to distinguish between several possible formation mechanisms. The physical nature of the precursors, especially grain size, must affect the textures of the chondrules they yield when heated. We melted precursors of different grain sizes, including extremely fine-grained crystalline aggregates analogous to nebular condensates, to see whether objects resembling most natural chondrules can be crystallized. With one-minute heating and moderate cooling rates, the grain size of the charges depends directly on the grain size of the starting material, for temperatures up to very close to the liquidus temperature. A single rapid heating of condensate-like material thus produces very fine-grained chondrules, like dark-zoned chondrules, for a very wide range of peak temperatures. It is incapable of generating the observed textural distribution of chondrules, which are predominantly porphyritic. The simplest model for chondrules, a single heating of unmodified condensate material, therefore appears unrealistic. Coarse-grained chondrules might be formed from fine-grained precursors by extended heating with evaporation leading to coarsening, or by multiple reheating events, with higher temperatures in subsequent events. Otherwise an origin from annealed condensates, planetary rocks, or by condensation of liquid and crystals is required.

1. INTRODUCTION

The abundance of chondrules in chondritic meteorites, and of asteroids with spectra resembling those of chondrites, suggests that the production of tiny melt spheres was an important process in the early solar system. Whether this was an astrophysical or planetary process is of major concern, and is not fully resolved despite much effort (e.g., Hewins et al., 1996). The melt spheres must have been produced by the condensation of vapor or by the melting of preexisting solids. Evidence for condensation exists only for specific cases (Krot et al., 2003), and the provenance of the solid precursors of most chondrules has been a subject of great interest. A popular idea has been that the melting of nebular or possibly circum-stellar condensates, consequently of very fine-grained solids (Taylor et al., 1983; Grossman, 1988; Hewins, 1997). Indeed Clayton (1980) even proposed that chondrule precursors were chemically unequilibrated aggregates of circum-stellar oxides rather than silicates.

The physical nature of the precursors has consequences for the properties of the chondrules they yield. Connolly et al. (1998) examined synthetic chondrule textures and found a correlation between grain size of starting material and size of resulting olivine phenocrysts after (incomplete) melting and crystallization. In this study we examine the melting of extremely fine-grained crystalline aggregates, to see whether the resulting melt spheres can crystallize to produce textures comparable to those of most natural chondrules. Failure to duplicate the textures would eliminate the single heating of unmodified condensate material, probably the simplest model for the origin of chondrules.

2. EXPERIMENTAL TECHNIQUES

Dynamic crystallization experiments were carried out in a DelTech DT-31-VT-OS muffle tube furnace, using Pt wire loops to support the sample and water-quenching. Mixing of CO-CO_2 provided an atmosphere with an oxygen fugacity of IW-0.5, as measured with a Corning yttria-stabilized zirconia electrolyte cell. A type S thermocouple wire (Pt100-Pt90/Rh10) placed 5 mm above the sample was used to monitor temperature. This was calibrated against the melting point of Pd (1554°C).

We varied grain size of starting material, peak temperature (mostly 1460–1620°C) and heating time (1–120 min.) independently to determine the influence of each on texture. To minimize the effect of different cooling rates on dissolution and growth of crystals, we used the same cooling sequence for all runs. We approximated a natural cooling curve in a similar way to Yu and Hewins (1998), using the programmed steps shown in Table 1 and Figure 1.

Starting materials differed principally in the grain size of their olivine. Brazil forsterite ($Fo_{94.4}$) was crushed and ground using an onyx mortar and pestle and sieved to between 20 and 45 μm. San Carlos ($Fo_{90.2}$) olivine was passed through the finest size sieve and was less than 20 μm. To obtain finer grained material, we used forsterite ($Fo_{100.0}$) synthesized by a sol-gel process. This process (Jones et al., 1997) involves the reaction of Mg with methanol, subsequent addition of tetraethoxysilane, and then the use of an aqueous solution of hydrogen peroxide as a hydrolyzing agent. Once the solvents are removed, a xerogel is produced. This xerogel was heated in a moist environment as described by Burlitch (pers. comm.) to remove volatiles including carbon and convert it to crystalline olivine. Some sintering and agglomeration of the forsterite occurs upon heating, producing a heterogeneous mixture of particles ranging in size from grains of several microns to friable clumps near 100 μm. There is no evidence of these clumps surviving partial melting and we assume that when melt first formed it contained 1–3 μm olivine relicts.

Each starting material included 60% of one of the forms of olivine mixed with crushed crystalline diopside (25%) and albite (15%), to prepare 40 mg pellets of type IA/IAB chondrule analogues. Their bulk compositions are listed in Table 2 and shown in Figure 2. They lie just outside the cluster of Semarkona type IAB chondrules of Jones (1994) in Figure 2 but are closer to the IAB mean composition than to the IA mean composition (Jones and Scott, 1989). They would probably crystallize some pyroxene with a lower cooling rate than used here. Table 2 also shows their calculated liquidus temperatures, based on Herzberg (1979), which vary with the Fe/Mg of the olivine used. The inferred olivine disappearance temperatures for two-hour runs are probably a better guide to the true liquidus temperatures. However, they are influenced by grain size as well as composition, and longer times might give slightly lower estimates for the coarser mixtures.

* Author to whom correspondence should be addressed (hewins@rci.rutgers.edu).

Table 1. Cooling steps from peak temperature.

RATE(°C/hr)	TIME(min.)	ΔT(°C)
2400	4	160
1440	4	96
720	6	72
480	6	48
360	15	90
TOTAL	35	466

As chondrule textures depend primarily on the number of nuclei available during cooling (Lofgren, 1996), the number density of crystals is a sensitive indicator of the intensity of melting, in terms of destruction of nuclei. We therefore used the number of crystals per unit area in BSE images made on a JEOL 8600 electron probe as a basis of comparison between synthetic and natural chondrules, because it is less arbitrary and more quantitative than using texture. The range of number densities in our charges is about 4 to 40000/mm^2. Thus it is practical to count the entire section for the coarsest grained charges. For the finer grained charges we chose representative regions as free of vesicles as possible. We stress that we use the number densities measured in a similar way for a series of samples not to discuss nucleation and crystal growth but only as a measure of the extent of melting. Because different portions of a charge may have different abundances of crystals (e.g., Connolly et al., 1998), the density on one surface may not be representative of the whole volume. Nevertheless, the internal consistency of our results, in terms of number density versus peak temperature, indicates that heterogeneities in the fine grained charges are not a serious problem.

To make the number densities more accessible, they were converted into a nominal grain size (Hewins et al., 1997). There are gradations between textural types making it hard to classify textures unambiguously, (e.g., Connolly et al., 1998). We therefore use nominal grain sizes of 100, 40 and 10 μm as the boundaries between barred, porphyritic, microporphyritic and crytoporphyritc (microporphyritic visible in BSE but not in PPL) olivine textures. This eliminates arbitrary choices when plotting texture maps. These divisions between BO, PO, MPO and CPO were chosen for natural chondrules, to make most type IA chondrules (Jones and Scott, 1989) classify as MPO and most type IIA as PO (Hewins et al., 1997). Cryptoporphyritic textures are similar to microporphyritic in BSE, but too fine-grained to be identified as such in thin sections. Some charges with porphyry textures transitional to BO (Connolly et al., 1998), elongate or platy hopper olivine porphyry, are counted as BO in texture maps using the 100 μm criterion. This is not of concern as even with these included "BO" textures are found only for a very restricted peak temperature interval.

High resolution images of the charges were made using a JEOL JSM 840A SEM at the Université Paris VI, and enhanced using Adobe Photoshop. All BSE images used here were taken at a magnification of

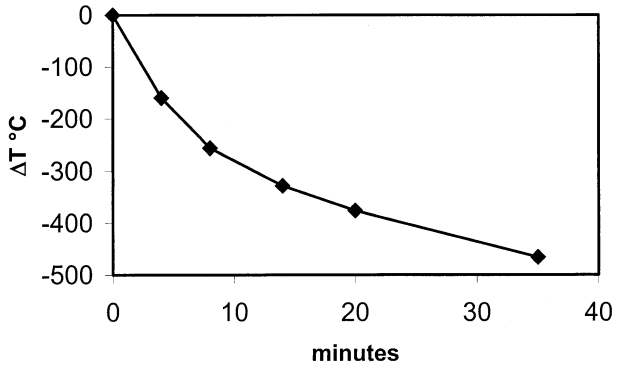

Fig. 1. Cooling path experienced by all charges, after heating for one minute at their various peak temperatures.

Table 2. Bulk Compositions* of Starting Material.

Mixture with	1. Brazil Fo	2. San Carlos	3. pure Fo
grain size μm	20–45	0–20	1–3
SiO_2	50.71	49.38	50.52
TiO_2	0.09	0.05	0.05
Al_2O_3	5.74	5.72	5.72
FeO	3.78	6.13	0.40
Cr_2O_3	0.01	0.01	0.01
MnO	0.25	0.02	0.02
MgO	35.68	32.14	36.86
CaO	3.87	3.85	3.82
Na_2O	2.85	2.85	2.85
K_2O	0.07	0.07	0.07
TOTAL	102.05	100.21	100.12
olivine out, 2hr	1590	1580	1610
calc.liquidus °C	1622	1591	1632

* Calculated from electron microprobe analyses of the minerals used (Fox, 2002; Connolly, 1996).

×500 and represent 200×200μm squares. Details of all charges are noted in Table 3. Supplementary experiments are reported in Fox (2002).

3. RESULTS

3.1. Starting Material with 20–45μm Olivine

Typical textures of recovered charges are shown in Figure 3, for a very small range of peak temperatures between (1575 and 1588°C) and heating times between 1 and 90 min at peak temperature. These show a transition from partial to almost complete melting, resulting in porphyritic to barred olivine texture (cf. Connolly et al., 1991). For initial temperatures a little above this range, totally glassy charges were found, though our furnace could not reach temperatures sufficient to melt this material completely with one-minute heating. Many of the coarser olivine crystals show fractures, which tend to continue into the glass but be fainter there. These fractures are much less regular than those seen in inverted protopyroxene. The cause of these cracks is unknown. Micrographs of the

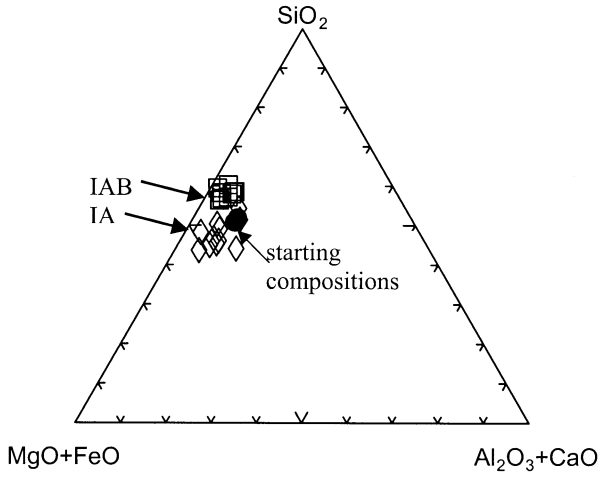

Fig. 2. Bulk compositions of starting materials (filled circles), compared to (diamonds) Semarkona type IA chondrules (Jones and Scott, 1989) and (squares) type IAB chondrules (Jones, 1994).

Table 3. Peak Heating Conditions and Nominal Grain Sizes (NGS) for all Charges.

Sample	Time(min)	Temp(°C)	NGS(μm)	Sample	Time(min)	Temp(°C)	NGS(μm)
Starting Material With 20–45μm Brazil Olivine							
V2	60	1588	117	V10	120	1583	316
V3	1	1615	67	V11	1	1600	110
V4	15	1616	glass	V12	1	1575	52
V5	90	1585	408	V13	1	1542	46
V6	30	1584	72.3	V14	1	1500	40
V7	30	1599	glass	V15	1	1476	43
V8	30	1613	glass	V16	1	1473	36
Starting Material With 0–20μm San Carlos Olivine							
DZ2	1	1600	412.6	T3	30	1599	422
DZ3	1	1575	44.6	T4	90	1585	glass
DZ4	1	1559	37.7	T5	60	1589	glass
DZ5	1	1525	33.0	T6	1	1612	393
DZ6	1	1495	18.8	T7	30	1586	331
DZ7	1	1470	17.8	T8	1	1614	glass
T1	120	1589	glass	T9	30	1614	glass
T2	12	1602	glass	T10	15	1614	glass
Starting Material With 1–3μm Sol-Gel Olivine							
DZ′2	1	1600	7.9	Y1	30	1614	395
DZ′3	1	1575	7.8	Y3	1	1612	41
DZ′4	1	1542	7.2	Y2	1	1607	38
DZ′6	1	1500	5.4	X5	120	1589	29
DZ′7	1	1476	5.9	X4	30	1586	15
DZ′5	1	1472	5.5	X3	90	1585	25
Y4	15	1613	175	X2	12	1602	23
Y5	30	1599	260	X1	60	1589	49

charges with the lowest peak temperatures are shown below, in a comparison with those for the other starting mixtures.

Figure 4 is a map of the textures of all the charges from this starting material, shown as a function of peak temperature and time at peak temperature. Textural fields are drawn using the nominal grain size values, which are indicated on the figure for each charge. Most of the charges are porphyritic, with finer-grained porphyries (MPO) at lower temperatures, below 1500°C, and coarser above 1580°C. Because of chance effects relating to survival of nuclei and embryos, texture maps such as those shown here usually show some overlap of textural fields, e.g., as in Stolper and Paque (1986). The field boundaries can be located to within about 20°C in Figure 3, and with finer grained starting material to less than 10°C. The PO field is about 140°C wide. The olivine disappearance temperature falls as expected with heating time and we can estimate the liquidus (as 1590°C) from the disappearance temperature for two hours (Hewins and Connolly, 1996). The BO field is less than 20° wide.

3.2. Starting Material with 0–20μm Olivine

Figure 5 shows some of the textures produced from starting mixture 2 with olivine finely ground and passed through the

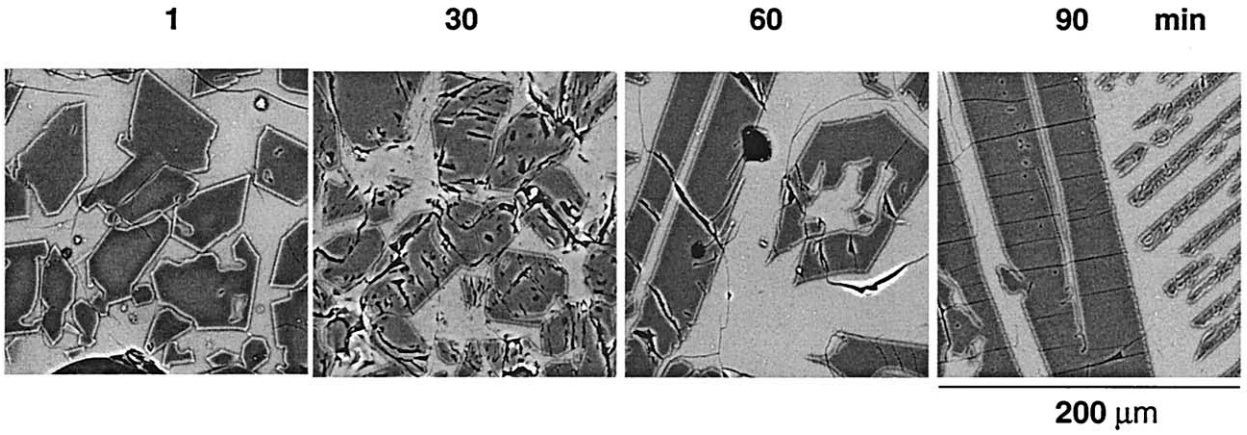

Fig. 3. Effect of heating time at approximately 1580°C (before normal cooling) on charges prepared from starting material with 20–45 μm olivine: textures coarsen from porphyritic olivine to barred olivine. The charges are V12, V6, V2 and V5. In this and all similar figures, the BSE images are 200×200 μm, dark grey is olivine, light grey is glass, black is vesicles and cracks, and white is surface contamination and charging.

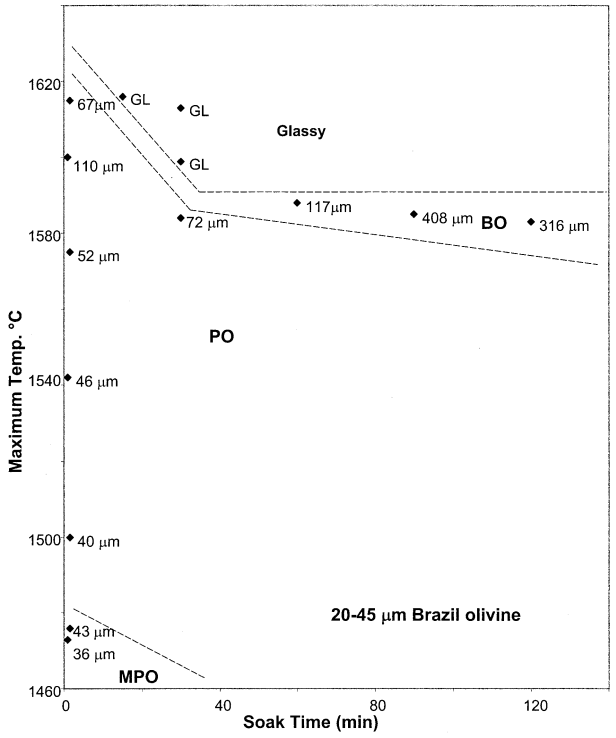

Fig. 4. Map of textures of charges prepared from starting material with 20–45 μm olivine, as a function of peak temperature and time at peak temperature. In this and all similar figures, the texture fields are glassy, barred olivine, porphyritic olivine, microporphyritic olivine and cryptoporphyritic olivine; and the numbers beside each experiment are nominal grain sizes in μm derived from the number of crystals per unit area.

smallest sieve mesh size available. Because of the effect of both temperature and time on olivine dissolution, for short peak heating times, equivalent textures plot on diagonal lines in this figure. Only one of the many glass charges was imaged. The textures of the barred olivine crystals resemble in detail those produced by Faure et al. (2003). Micrographs of the lowest temperature charges are shown below.

The textures of all the charges are mapped in Figure 6. The boundary between glass and BO is similar to the one in Figure 4 and the BO field is about 20° wide. The nominal grain size increases systematically with heating temperature, in a more striking way than for the coarse starting mixture (Fig. 3). The biggest difference from the results with the coarser starting material is that the PO field is now only about 20° wide, and the field of MPO is much larger, extending to within 40° of the olivine-out curve.

3.3. Starting Material with Sol-Gel Olivine

The mixture using the very fine-grained olivine produced by the sol-gel process yields the textures shown in Figure 7. Charges kept at peak temperature for one minute are much finer grained (CPO) than the runs at the same temperatures for the coarser starting materials. However, they are coarser with increased peak temperature, becoming more truly porphyritic. Fe-Mg zonation in interstitial liquid, as well as in olivine, is present in the charges. It is especially evident in CPO charges, particularly in small pockets of glass interstitial to clusters of fine crystals. Charges held at the same peak temperatures for longer times before cooling also exhibit coarsening, becoming barred in the limit. A peculiarity of the BO charges is fractures crossing the olivine plates, but not the intervening glass.

Vesicles are prominent in the lower temperature charges, some of which are shown below, until nominal grain size is about 40 μm when these charges are not more vesicular than those of the coarser starting mixes discussed above. Vesicle abundance decreases with higher peak temperatures and longer heating times. Their presence reflects the fact that it is difficult for bubbles to migrate when trapped between fine crystals (Maharaj and Hewins, 1998) and not differences in the compositions of the starting materials.

The texture map with NGS values for the third starting mixture is shown in Figure 8. The curve for total melting could not be determined because the temperatures for this Fe-free material are too high, but the BO field is expected to be similar to that of Figure 6. Though the general pattern of fields is similar to what was seen above, the PO and MPO fields are shrunk, each being only about 10° wide. For any temperature up to within about 40° of the olivine disappearance curve, the texture is cryptoporphyritic.

4. DISCUSSION

4.1. Effect of Grain Size of Starting Material

Connolly et al. (1998) investigated the effect of precursor grain size on chondrule textures, with particular emphasis on

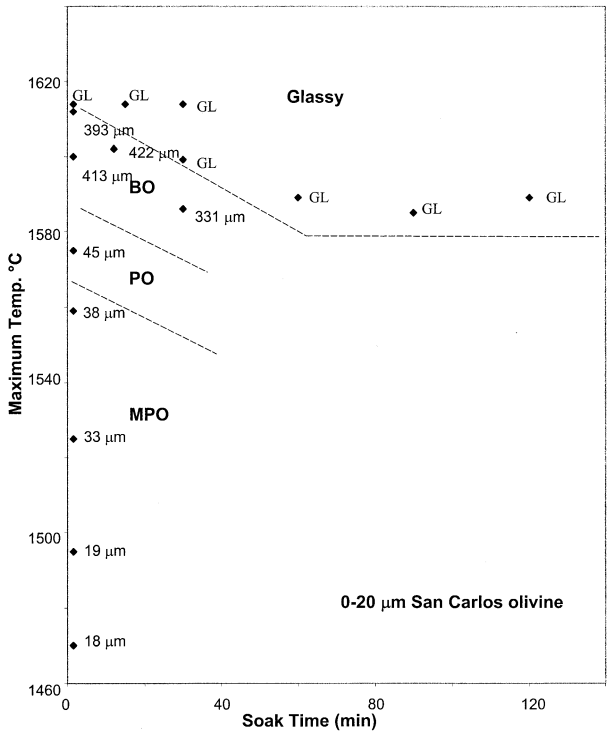

Fig. 6. Map of textures of charges prepared from starting material with 0–20 μm olivine, as a function of peak temperature and time at peak temperature.

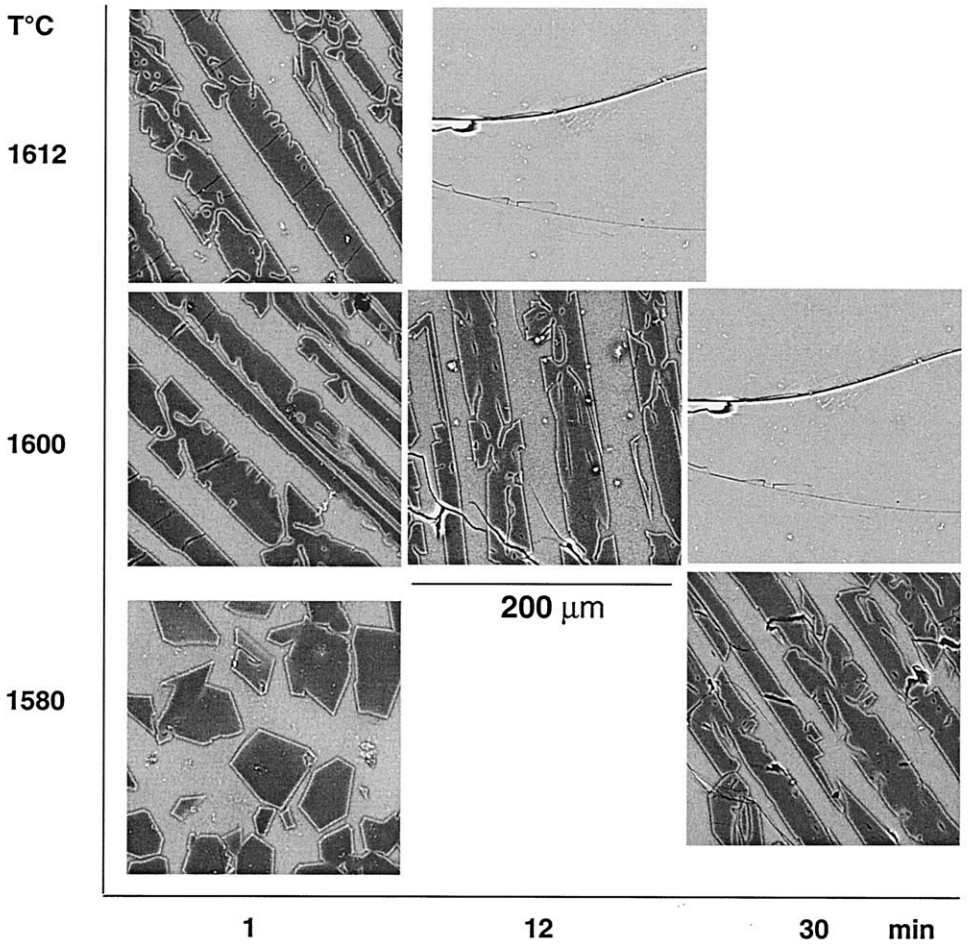

Fig. 5. Textures shown for approximate peak temperatures and heating times on charges prepared from starting material with 0–20 μm olivine. The charges shown are, from the top left, T6, T10 (but T3 is used as a proxy for T10), DZ2, T2, T3, DZ3 and T7.

the effect of very coarse-grained starting material. They found that a coarse-grained mix raised to peak temperature and immediately cooled could produce chondrule textures, particularly barred olivine textures, with peak temperatures well above the liquidus, because the time needed for dissolution of olivine and elimination of nuclei is long. They also showed that as the grain size of the starting material became finer, the field for porphyritic texture was reduced to a very small range of peak temperatures, though microporphyritic textures were present. This paper provided the motivation for the present study, which aimed to find out whether typical chondrule textures could be produced with extremely fine-grained starting material.

We summarize the results of the present study in Figure 9, which is a time-temperature texture map comparing especially the higher temperature runs. It shows that the textures developed with the three different starting materials are very similar for a given heating time, provided that the effect of different liquidus temperatures is taken into account. The temperature shown in Figure 9 is ΔT relative to the olivine disappearance temperatures estimated from Figures 3, 6 and 8. Temperatures of complete melting decrease by nearly 40°C as heating time is increased from 1 min to 2 h. The boundaries in this figure are the mean positions of the field limits. The BO field is about 20°C wide and corresponds approximately to the zone where nuclei are destroyed but embryos of sufficient size remain to graduate to nuclei for our cooling curve (Lofgren, 1996). Below the BO/PO boundary the presence of equant solid crystals indicates survival of nuclei and in the case of the second mix with San Carlos olivine, relict ferroan olivine is observed inside phenocrysts in some cases.

For the low temperature runs the textures are very different for the three starting materials, as can be inferred from the NGS values shown in Figures 4, 6 and 8. These textures are compared in Figure 10. The charges are predominantly cryptoporphyritic for the finest grained starting material, microporphyritic for the intermediate, and porphyritic for the coarsest starting material (Fig. 10). For every peak temperature, a coarser starting mixture gives a coarser final texture. Figure 11 shows curves for the coarsening of each mixture as peak temperature increases. There is very little difference in size of crystals for a given composition up to the (*two hour*) olivine disappearance temperature (Fig. 11): apparently heating only reduces the size of most crystals and they grow back during cooling. After that, significantly more crystals are totally dis-

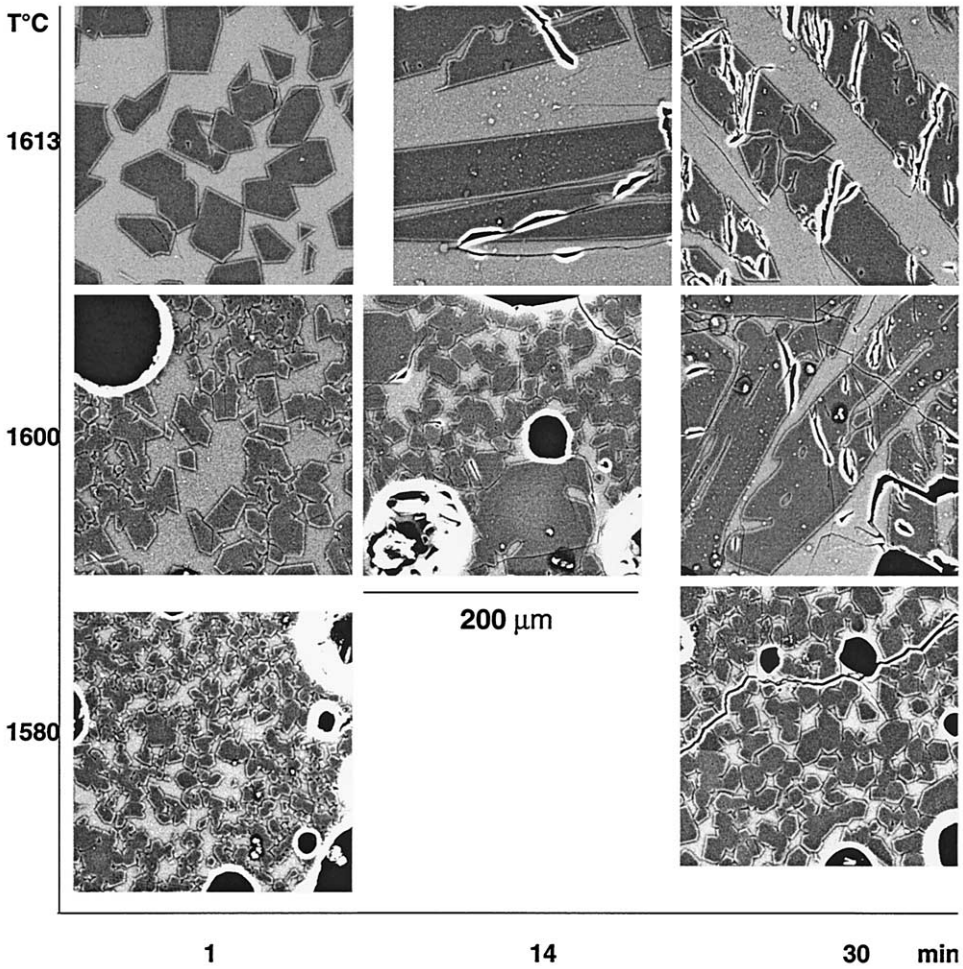

Fig. 7. Textures shown for approximate peak temperatures and heating times on charges prepared from starting material with olivine from gel. The charges shown are, from the top left, Y3, Y4, Y1, DZ'2, X2, Y5, DZ'3, X4.

solved in the time at peak temperature, leading to coarser textures after cooling and growth. A consequence of this is that for a range of peak temperatures, chondrule textures will depend mainly on the grain size of their precursors, for similar rapid heating conditions.

In Figure 12, we show nominal grain sizes for all the charges kept at peak temperature for one minute. This figure confirms the tendency demonstrated by Connolly et al. (1998) for the PO field to have a smaller extent in peak temperature for a smaller precursor grain size, though because of different thermal histories we cannot make a direct comparison of the two sets of experiments. We were unable to melt the mix with the Fo gel sufficiently in one minute to generate BO texture, but by extrapolation from the longer runs the PO field can only be about 5° wide. The MPO field also pinches down to about 5° wide for the finest grained starting material, an effect not observed in earlier work where coarser mixes were used. The nature of the textures depends critically on the grain size of the starting material and the typical chondrule textures could not be derived from very fine-grained precursors unless the peak temperature were fixed within about ± 10°C of the liquidus. We argue below that normal PO and MPO textures could not be derived in a single heating event starting with fine-grained precursors such as condensates.

4.2. Chondrule Formation Models

Liquid forms either by the condensation of a gas or the melting of solids and, extending the ideas of Taylor et al. (1983) and Grossman (1988), chondrules may form in either nebular, asteroidal/planetary or near-solar/extra-nebular environments. With the present experiments we can examine only the possibility of formation of chondrules by melting solids. If chondrules formed by melting, the precursor solids may have been mineral clusters, clumps or dustballs (Nagahara, 1983; Grossman, 1988; Wood, 1996). The diversity of chondrule compositions has been explained by chemical fractionation of nebular condensates before chondrule formation (Taylor et al., 1983; Grossman et al., 1988), as well as by partial evaporation during melting of nebular condensates (Hewins et al., 1997; Cohen et al., 2000, in press; Yu et al., 2003). Precursor condensate dustballs might be aggregates of fine-grained crystals similar to those in chondrite matrix (e.g., Brearley, 1996), i.e., about 1 μm in size. The nature of any chondrules produced by

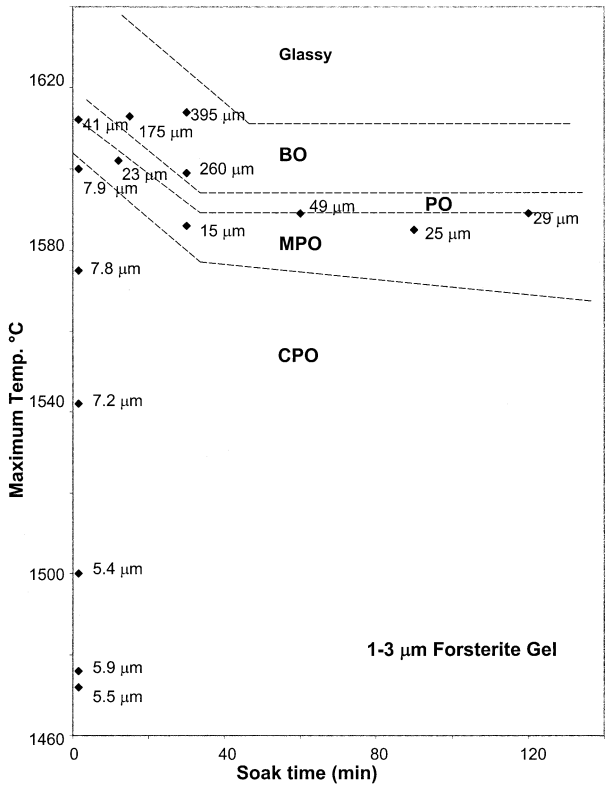

Fig. 8. Map of textures of charges prepared from starting material with gel olivine, as a function of peak temperature and time at peak temperature.

melting solids will depend on a number of factors, in particular their grain size (Connelly et al., 1998) and heating time. Heating times are a matter of seconds in some models, such as lightning and impact, but of hours for nebular shock wave heating (Desch and Connolly, 2002).

We have focused our present experiments on the model of chondrule formation by rapid heating of aggregates of fine-grained nebular or circumstellar condensates, using 1 min for the time at peak temperature. We find a very close resemblance between chondrule grain size and precursor grain size over a wide range of temperatures (Fig. 11). Connolly et al. (1998) concluded that microporphyritic chondrules required precursors <63 μm in size, which we can redefine as <20 μm (Fig. 11, 12). If we consider precursors of a few microns which might represent nebular condensates, the implications are quite clear and confirm the general predictions of Connolly et al. (1998): the crystals that grew on cooling would generally be <10 μm (Figs. 8, 11). For a wide range of peak temperatures, such a process would result in very fine-grained chondrules, similar perhaps to cryptoporphyritic (Hewins et al., 1997) or dark-zoned chondrules (Dodd and Van Schmus, 1971). Such chondrules are relatively uncommon and are not listed in the abundance tables of Gooding and Keil (1981) and Grossman et al. (1988). Clearly it would be impossible to produce the commonest chondrule textures, PO and MPO, in the abundance in which they are observed (Gooding and Keil, 1981; Grossman et al., 1988), for any reasonable distribution of peak temperatures and/or liquidus temperatures, in a single rapid heating event. The common chondrules would require a different origin than the fine-grained ones.

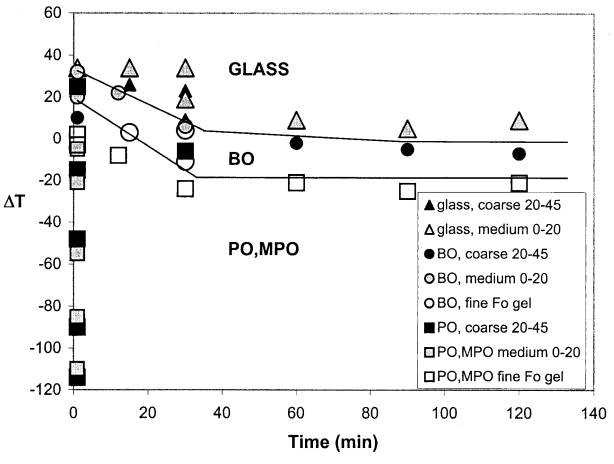

Fig. 9. Comparative map of textures for all starting materials. Peak temperature is given relative to olivine disappearance temperature for two hours at peak temperature.

We conclude that porphyritic chondrules were not generated by melting fine-grained condensates. Certainly those grains surviving as relics in chondrules were not fine, whether they were formed as condensates (Grossman, 1988) or in older chondrules (Alexander, 1996) or were asteroidal in origin. Note that the present arguments based only on textures cannot exclude the possibility that the precursors could have been coarse-grained rocks melted in a planetary setting. An asteroid belt in which large planets accreted and then were removed by gravitational perturbations (Chambers and Wetherill, 2001) is an environment where large impacts producing melt droplets might be common. It has also been proposed that chondrules were produced in planetesimals heated by short-lived isotopes (Chen et al., 1998; Lugmair and Shokolyukov, 2001). Whether any of these alternatives could explain most chondrules was not answered in Hewins et al. (1996) and cannot be resolved here.

A planetary origin for chondrules to give the necessary coarse-grained precursors is not required, however: chondrules might have been made from nebular condensates that were annealed to varying extents in the solar nebula. They perhaps resembled amoeboid olivine inclusions, which have been observed inside chondrules in rare cases (Komatsu et al., 2001; Yurimoto and Wasson, 2002). Moreover, the classic model with fine condensates as immediate precursors to chondrules is not necessarily ruled out, if the thermal history is very different from that used in the present experiments. Though not observed in the present study, in long-duration low-pressure isothermal experiments where evaporation was important, Ostwald ripening or coarsening was observed (Cohen et al., 2000). Such conditions approximate the thermal history predicted by the shock wave model of Desch and Connolly (2002).

A final alternative is that, with less extended heating times, a more complex thermal processing might be effective, e.g., one involving recycling of chondrules ultimately derived from condensates. Indeed Alexander (1996) proposed that chondrules and their debris were the precursors to chondrules found in ordinary chondrites: essentially all chondrules might have

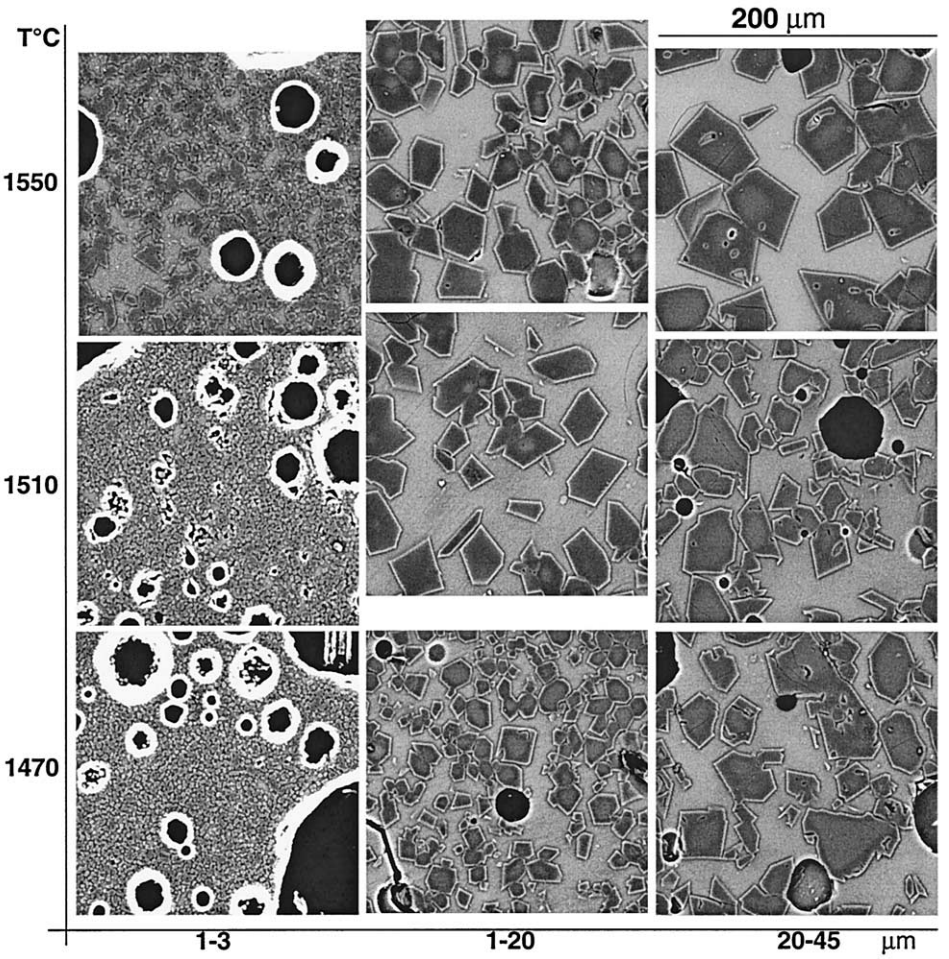

Fig. 10. Textures for the three starting materials with different grain sizes, after *one minute* heating at low peak temperatures and continuous cooling. The charges shown are, from the top left, DZ44, DZ'6, DZ'7, DZ4, DZ5, DZ7, V13, V14, V16.

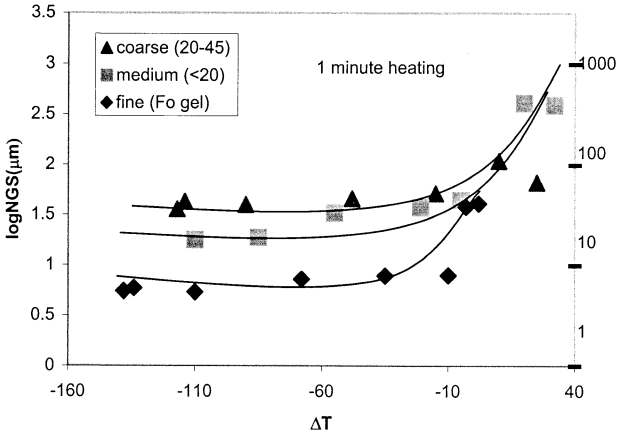

Fig. 11. Coarsening curves: response of the different compositions to peak heating temperature (ΔT relative to the olivine disappearance temperature) as a function of grain size of starting materials.

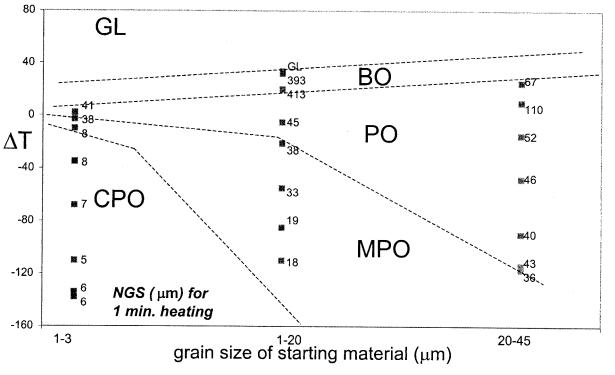

Fig. 12. Texture map for charges which spent 1 min. at peak temperature, as a function of peak temperature (relative to two-hour olivine disappearance temperature) and grain size of starting mix.

been recycled. Fox (2002) and Fox and Hewins (2002, 2003) showed that reheating a fine-grained porphyritic chondrule generates a coarser texture, to the extent that the second heating is at a higher temperature than the first. The fraction of porphyritic chondrules produced with a given range of peak temperatures is greater if the precursor is coarser-grained and that can be achieved by melting a chondrule a second time at a higher temperature than it was heated the first time. These experiments supporting the idea of fine-grained condensates as the ultimate precursors of chondrules will be reported in detail elsewhere.

5. CONCLUSIONS

1. A single rapid heating event is expected to convert very fine-grained aggregates, e.g., condensates, into fine-grained chondrules, like dark-zoned chondrules, and is incapable of generating the observed textural distribution of chondrules, which are predominantly porphyritic.
2. Coarse-grained chondrules might be formed from fine-grained precursors with a different thermal history from that assumed here. Extended heating at low pressure or multiple reheating events, with higher temperatures in subsequent events, could convert fine-grained precursors into chondrules with an appropriate distribution of textural types.
3. Chondrule texture distributions could perhaps also be reconciled with other possibilities such as formation of chondrules as liquid-solid condensates or impact melt droplets.

Acknowledgments—We thank Harold Connolly and Yang Yu for help with experimental techniques, and J. M. Burlitch, J.A. Nuth III and L.C. Klein for providing various starting materials. Omar Boudouma is thanked for the warm welcome in his lab and for his expertise with the SEM. Discussions with G.E. Lofgren were valuable throughout the course of this study. Critical reviews by Harold Connolly and someone who did not précise his name led to considerable improvements to the paper. This work was supported by NASA grants NAG5-4475 and 5-10495.

Associate editor: C. Koeberl

REFERENCES

Alexander C. M. O'D. (1996) Recycling and volatile loss in chondrule formation. In *Chondrules and the Protoplanetary Disk* (eds. R. H. Hewins, R. H. Jones, and E. R. D. Scott), pp. 233–242. Cambridge Univ. Press, Cambridge.

Chambers J. E. and Wetherill G. W. (2001) Planets in the asteroid belt. *Meteor. Planet. Sci.* **36,** 381–399.

Chen J. H., Papanastassiou D. A., and Wasserburg G. J. (1998) Re-Os systematics in chondrites and the fractionation of the platinum group elements in the early solar system. *Geochim. Cosmochim. Acta* **62,** 3379–3392.

Clayton D. D. (1980) Chemical energy in cold-cloud aggregates: The origin of meteoritic chondrules. *Astrophys. J.* **239,** L37–L41.

Cohen B. A., Hewins R. H., and Yu Y. (2000) Evaporation in the young solar nebula as the origin of "just-right" melting of chondrules. *Nature* **406,** 600–602.

Cohen B. A., Hewins R. H. and Alexander C. M. O'D. (in press) The formation of chondrules by open-system melting of nebular condensates. *Geochim. Cosmochim. Acta* **68**.

Connolly H. C. Jr. (1996) The complicated nature of chondrule formation: an experimental investigation into the melting and precursor history of chondrules. Ph.D. thesis, Rutgers University, 185 pages.

Connolly H. C. Jr. and Hewins R. H. (1991) The influence of bulk composition and dynamic melting conditions on olivine chondrule textures. *Geochim. Cosmochim. Acta* **55,** 2943–2950.

Connolly H. C. Jr., Jones B. D., and Hewins R. H. (1998) The flash melting of chondrules: an experimental investigation into the melting history and physical nature of chondrule precursors. *Geochim. Cosmochim. Acta* **62,** 2725–2735.

Desch S. J. and Connolly H. C. Jr. (2002) A model for the thermal processing of particles in solar nebula shocks: application to cooling rates of chondrules. *Meteorit. Planet. Sci.* **37,** 183–208.

Dodd R. T. and Van Schmus W. R. (1971) Dark-zoned Chondrules. *Zeits. Chem. Erde, Band.* **30, Heft1/4,** 59–69.

Faure F., Trolliard G. and Soulestin, B. (2003) TEM investigation of forsterite dendrites. *Am. Mineral.* **88,** 1241–1450.

Fox G. E. (2002) Chondrule synthesis using fine-grained precursors. Ph.D. thesis, Rutgers University, 152 pages.

Fox G. E. and Hewins R. H. (2002) Nebular condensates, chondrules and recycling. *Lunar Planet. Sci.* **XXXIII** No. 1612.

Fox G. E. and Hewins R. H. (2003) Chondrule recycling experiments. *Meteor. Planet. Sci.* **38,** A.

Gooding J. L. and Keil K. (1981) Relative abundances of chondrule primary textural types in ordinary chondrites and their bearing on conditions of chondrule formation. *Meteor.* **16,** 17–43.

Grossman J. N. (1988) Formation of chondrules. In *Meteorites and the Early Solar System* (eds. J. F. Kerridge and M. S. Matthews), pp. 680–696. University of Arizona Press, Tucson.

Grossman J. N., Rubin A. E., Nagahara H., and King E. A. (1988) Properties of chondrules. In *Meteorites and the Early Solar System* (eds. J. F. Kerridge and M. S. Matthews), pp. 619–659. University of Arizona Press, Tucson.

Herzberg C. T. (1979) The solubility of olivine in basaltic liquids: an ionic model. *Geochim. Cosmochim. Acta* **43,** 1241–1251.

Hewins R. H. (1997) Chondrules. *Ann. Rev. Earth Planet. Sci.* **25,** 61–83.

Hewins R. H. and Connolly H. C. Jr. (1996) Peak temperatures of flash-melted chondrules. In *Chondrules and the Protoplanetary Disk* (eds. R. H. Hewins, R. H. Jones, and E. R. D. Scott), pp. 197–204. Cambridge University Press.

Hewins R. H., Jones R. H., and Scott E. R. D. (1996) Chondrules and the Protoplanetary Disk. Cambridge University Press, 346 pp.

Hewins R. H., Yu Y., Zanda B., and Bourot D. M. (1997) Do nebular fractionations, evaporative losses or both, influence chondrule compositions? *Antarct. Meteor. Res.* **10,** 275–298.

Jones R. H. (1994) Petrology of FeO-poor, porphyritic pyroxene chondrules in the Semarkona chondrite. *Geochim. Cosmochim. Acta* **58,** 5325–5340.

Jones R. H. and Scott E. R. D. (1989) Petrology and thermal history of type IA chondrules in Semarkona (LL3.0). *Proc. 19th Lunar Planet. Sci. Conf.* 523–536.

Jones S. A., Wong S., Viswanathan S., Kohlstedt D. L., and Burlitch J. M. (1997) Sol-gel synthesis and characterization of magnesium silicate thin films. *Chem. Mater.* **9,** 2567.

Komatsu M., Krot A. N., Petaev M. I., Ulyanov A A., Keil K., and Miyamoto M. (2001) Mineralogy and petrography of amoeboid olivine aggregates from the reduced CV3 chondrites Efremovka, Leoville and Vigarano: Products of nebular condensation, accretion and annealing. *Meteor. Planet. Sci.* **36,** 629–641.

Krot A. N., Libourel G., Goodrich C. and Petaev M. I. (2003) Silica-rich igneous rims around magnesian chondrules in carbonaceous chondrites: evidence for fractional condensation during chondrule formation. *Geochim. Cosmochim. Acta* **67,** submitted.

Lofgren G. E. (1996) A dynamic crystallization model for chondrule melts. In *Chondrules and the Protoplanetary Disk* (eds. R. H. Hewins, R. H. Jones, and E. R. D. Scott), pp. 187–196. Cambridge University Press, Cambridge.

Lugmair G. W. and Shukolyukov A. (2001) Early solar system events and timescales. *Meteor. Planet. Sci.* **36,** 1017–1026.

Maharaj S. V. and Hewins R. H. (1998) Chondrule precursor minerals as anhydrous phases. *Meteor. Planet. Sci.* **33,** 881–887.

Stolper E. and Paque J. (1986) Crystallization sequences of Ca-, Al-rich inclusions from Allende: The effects of cooling rate and maximum temperature. *Geochim. Cosmochim. Acta* **50,** 1785–1806.

Taylor G. K., Scott E. R. D., and Keil K. (1983) Cosmic setting for chondrule formation. In *Chondrules and Their Origins* (ed. E. A. King), pp. 262–278. Lunar and Planetary Institute, Houston.

Yu Y. and Hewins R. H. (1998) Transient heating and chondrule formation—evidence from Na loss in flash heating simulation experiments. *Geochim. Cosmochim. Acta* **62,** 159–172.

Yu Y., Hewins R. H., Alexander C. M. O'D., and Wang J. (2003) Experimental study of evaporation and isotopic mass fractionation of potassium in silicate melts. *Geochim. Cosmochim. Acta* **67,** 773–786.

Yurimoto H. and Wasson J. T. (2002) Extremely rapid cooling of a carbonaceous-chondrite chondrule containing very ^{16}O-rich olivine and a ^{26}Mg-excess. *Geochim. Cosmochim. Acta* **66,** 4355–4363.